# Absolute Beam Energy Measurements in $e^+e^-$ Storage Rings

M. Placidi
*CERN, Geneva, Switzerland*

**Abstract**

The CERN Large Electron Positron collider (LEP) has been dedicated to the measurement of the mass $M_Z$ and the width $\Gamma_Z$ of the $Z^0$ resonance during the LEP1 phase terminated in September 1995. The Storage Ring has been operated in *Energy Scan* mode during the 1993 and 1995 physics runs by choosing the beam energy $E_{\rm beam}$ to correspond to a CM energy at the IP's $E_{\rm CM}^{\rm peak} \pm 1762$ MeV. After a short review of the techniques usually adopted to set and control the beam energy this paper describes in more detail two methods adopted at LEP for precise beam energy determination, essential to reduce the contribution to the systematic error on $M_Z$ and $\Gamma_Z$. The positron beam momentum was initially determined at the 20 GeV injection energy by measuring the speed of a less relativistic proton beam circulating on the same orbit, taking advantage from the unique possibility of injecting the two beams into LEP at short time intervals. The positron energy at the $Z^0$ peak was in this case derived by extrapolation. Once transverse polarization became reproducibly available the Resonant Depolarization ($\underline{RD}$) technique was implemented at the $Z^0$ operating energies providing a $\leq 2 \times 10^{-5}$ instantaneous accuracy. $\underline{RD}$ Beam Energy Calibration has been adopted during the LEP Energy Scan campaigns as well as in Accelerator Physics runs for accurate measurement of machine parameters.

## INTRODUCTION

This paper is intended to give an overview of the several techniques which can provide information on the beam energy in Storage Rings and to account for the associated precisions.

Accurate knowledge of the beam energy is of relevant interest in storage rings dedicated to the measurement of the mass and the width of resonances. Reducing the uncertainty on the energy scale improves the quality of the determination of the resonance parameters since the energy information level sets the standard for the systematic contribution to the global error. Besides this specific issue on the energy scale calibration, the possibility of setting, monitoring and controlling the nominal energy of the accelerator with a high degree of reliability greatly improves the performance of the operation.

After a brief review of standard methods, which provide an energy information essentially derived from the measurement of the magnetic field in reference magnets or in the ring dipoles, the paper describes in detail more sophisticated techniques based on direct measurements of specific properties of beams like particle **velocity** and **polarization**.

The first method is based on the determination of the velocity of protons on a specific and reproducible orbit through a measurement of their revolution frequency. This provides the momentum per unit charge associated to that particular orbit which is the same for protons and leptons.

A second method, ($\underline{RD}$), by far the most accurate, measures the spin precession frequency of a vertically polarized beam, directly related to the average beam energy, by means of a controlled depolarizing resonance.

Other techniques involving special detectors or dedicated experiments are also accounted for to complete the review.

Experimental results from the 1995 LEP beam energy calibration campaign with $\underline{RD}$ are shown and effects responsible for changes in the CM energy at the IP's during the physics runs are described.

## STANDARD TECHNIQUES FOR ENERGY MONITORING

### The Integrating Coil

The usual method adopted to set the energy of a storage ring to some desired levels consists in measuring the *integrated magnetic field* $\int B\,ds$ in a Reference Magnet powered in series with the main ring dipoles. The information from a digital integrator connected to a long rotating coil properly positioned in the gap provides a continuous measurement of $\int B\,ds$ and is used as a reference for the current-regulated control of the main power converters. This is particularly important when the physics runs take place at energies different from the injection one and a magnet-cycling procedure is applied to compensate for hysteresis effects. The $\int B\,ds$ information is also part of the log-in data set provided at every fill to the experiments.

The reproducibility and the resolution of of this method referred to as *field display* ($\underline{FD}$) (1) are in the range of $\pm(20 \div 30)$ ppm.

For the field display to reproduce the situation represented by the dipoles in the accelerator tunnel the reference magnet should obey two basic rules i.e. **being structurally identical to the ring magnets and undergo the same environmental history** *. Temperature changes affect the nominal value of $\int B\,ds$ as they modify both the gap height and the length of the dipole cores: the $\underline{FD}$ technique provides information on the global effect.

The presence of a long coil in the magnet gap and the associated instrumentation together with the need of access for maintenance discourage the installation of the reference magnet in the tunnel itself, so the $\underline{FD}$ information requires other calibration techniques to be used as an absolute energy monitor.

*This includes essentially *temperature* changes, although in the case of the LEP dipoles, where the jokes are made of a mixture of steel laminations and concrete, other parameters like the *local humidity* are important to be monitored and controlled.

## The NMR Probes

Nuclear Magnetic Resonance probes provide a very precise measurement of the *local magnetic field* down to a $\sim 10^{-6}$ accuracy. Their compact volume allows for direct installation in the gap of the magnets with reduced interference with the vacuum chamber which provides on line monitoring of the time evolution of the dipolar field.

NMR probes do not provide information on the variations of the magnetic length with temperature and their use in a reference magnet should be associated to adequate temperature measurements in the accelerator tunnel.

The limitation of this information arises from the small number of sampled dipoles which requires good guarantees on the overall homogeneity both of the magnetic properties of the cores and of their thermal behavior.

## The LEP Flux-Loop System

The LEP reference magnet, made from a stack of standard dipole laminations, is installed in a temperature-controlled environment and series-connected with the main dipoles. Measurements of the integrated magnetic field are carried out with a flip coil mounted in the magnet gap along the position of the central orbit.

The LEP dipoles have iron-concrete cores which undergo aging and are sensible to both temperature and air humidity changes. The field-display information from the reference magnet is calibrated periodically by a direct measurement of the flux variations in an 8-fold loop consisting of electric wires mounted in the lower pole of each of the bending magnets and connected in series throughout each LEP octant (2) . The induced voltage from the flux variation in the loops when the whole dipole system undergoes a magnetic cycle of given excursion is measured by eight digital integrators in the even underground areas of the machine and provides a direct information on the $\int B\,ds$ along the accelerator from the dipoles in the actual environmental conditions. Polarity reversal permits a measurement of the remanent field which is of particular importance for the LEP low field dipoles.

The attainable accuracy in the determination of the beam momentum is of the order of $5 \times 10^{-4}$ since the method does not account for additional dipolar bending for orbits off-axis in the quadrupoles.

## THE NOMINAL ENERGY

For a given magnetic structure the **nominal energy** $E_0$ is defined for a beam circulating on the **central orbit** $C_0$ going in average through the center of the quadrupoles so that the bending strength experienced by the beam over a machine revolution comes only from the dipoles:

$$\frac{\beta E_0}{ec} = \frac{p_0}{e} = \frac{1}{2\pi} \oint_{C_0} B(s)\,ds \qquad (1)$$

The integration is extended over the central orbit $C_0$ defined by the central revolution frequency $f^0_{\rm rev}$:

$$f^0_{\rm rev} = \frac{\beta c}{C_0} = \frac{c}{h\ \lambda^0_{\rm RF}} \tag{2}$$

where $\lambda^0_{\rm RF}$ is the wavelength of the **nominal RF frequency** $f^0_{\rm RF}$ and $h$ the harmonic number.

## Measuring The Central Orbit

The nominal momentum of a beam off the central orbit in a FODO structure is modified by the additional integrated dipolar field in the quadrupoles according to Eq.1:

$$\Delta p = \frac{p_0}{\alpha_{\rm c}} \frac{\Delta C}{C_0} = \frac{e}{2\pi} \oint_C G(s)\, x(s)\, ds \tag{3}$$

where $\alpha_{\rm c}$ is the momentum compaction for the used optics, $G(s)$ the field gradient and $C = C_0 + \Delta C$ the length of the actual reference orbit. This effect modifies the betatron tunes (chromaticity) and generates closed orbit distortions induced by angular kicks from the (de)focusing strengths, which are minimum when the beam is centered.

In principle a direct method to define the central orbit would consist in looking for minimum orbit distortion (orbit differences) as a function of the RF frequency for different settings in the strength of the arc quadrupoles but the attainable accuracy is essentially limited by the associated tune shift.

The method commonly adopted in a regular FODO-lattice magnetic structure exploits the fact that in each magnetic cell the sextupoles are installed on the same girder as the quadrupoles and precisely aligned with respect to them. In this assumption a beam off-axis in the quadrupoles receives additional focusing from the same misalignment it has in the center of the sextupoles. This makes the betatron tunes $Q_{\rm x,y}$ depend on the sextupole excitation until the orbit is *on axis* in the quadrupole-sextupole complex.

The method then consists in measuring the dependence of the betatron tunes over the radial position of the orbit in the arcs by changing the RF frequency for different settings of the sextupole families i.e. for different chromaticities $Q' = \Delta Q / \Delta p/p$. For energy changes small compared to the acceptance of the machine the chromaticity varies linearly with the sextupole excitation and the lines $Q_{\rm x,y}(f_{\rm RF})$ will cross at one point defining the central RF frequency $f^0_{\rm RF}$.

If the particle velocity is known, as in the case of ultra-relativistic leptons, the method provides a measurement of the central orbit length $C_0$ (5).

Figure 1 shows an example of the use of positrons ($1 - \beta_{\rm e^+} \sim 3 \times 10^{-10}$) to

determine the length of the LEP **actual circumference** † from

$$C_0 = \frac{c\ \beta_{e^+} h_{e^+}}{f^0_{RF,e^+}} \tag{4}$$

The harmonic number $h_{e^+} = 31324$ gives $C_0^{LEP} = 26.658873$ km. The error in the circumference measurement is of the order of 0.3 mm corresponding to a relative error of about $1 \times 10^{-8}$. The accuracy on the frequency measurement is more than one order of magnitude better.

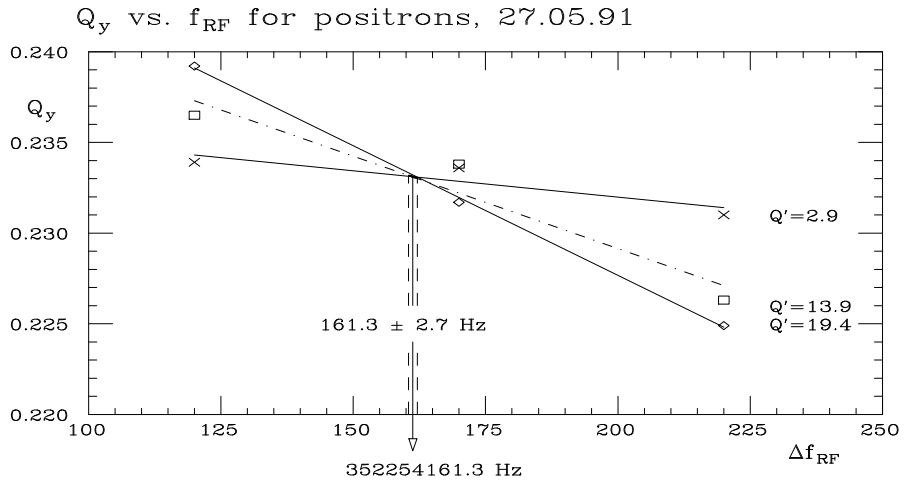


**Figure. 1**. *Positron* chromaticity measurements to determine the central revolution frequency and the length of the *central orbit*, ref.(5).

## THE CENTRAL MOMENTUM

The determination of the momentum on the central orbit requires the use of non ultra relativistic particles. Protons have been proposed (4) as their velocity $c\beta_p$ is measurably different from the speed of light.
After a measurement of the central orbit with positrons, following the method discussed above, protons are injected keeping the **same magnetic settings** and trapped by the RF system on a different harmonic number $h_p$ associated to the new velocity, determined from the knowledge of the nominal energy inferred from magnetic measurements.
A measurement of the chromaticity $Q'_p$ for different sextupole settings defines

† As stated in (3) the concept of *Terra ferma* has to be reconsidered when dealing with alignment stability in accelerators: the length of the central orbit is time-dependent due to seasonal and periodic ground motion as discussed in the last chapter.

the central RF frequency $f^0_{\mathrm{RF,p}}$ for protons and hence their velocity:

$$\beta_{\mathrm{p}} = \frac{C_0\, f^0_{\mathrm{rev,p}}}{c} = \beta_{\mathrm{e^+}} \frac{h_{\mathrm{e^+}}}{h_{\mathrm{p}}} \frac{f^0_{\mathrm{RF,p}}}{f^0_{\mathrm{RF,e^+}}} \tag{5}$$

The momentum competing to the **same central orbit** is common to positrons and protons

$$p_{\mathrm{e^+}} \equiv p_{\mathrm{p}} = c\beta_{\mathrm{p}} m_{\mathrm{p}} \gamma_{\mathrm{p}} = \frac{\beta_{\mathrm{e^+}} E_{\mathrm{e^+}}}{c} \tag{6}$$

within an accuracy

$$\frac{\Delta p}{p} = \gamma^2_{\mathrm{p}} \left( \frac{\Delta \beta}{\beta} \right)_{\mathrm{p}} \tag{7}$$

Figure 2 shows the application of this method to the determination of the central momentum for LEP at the nominal injection energy of 20 GeV (5). Due to the accuracy of the measurements the lines associated to the different chromaticities do not cross exactly at one point and an error ellipse for one standard deviation is shown on the figure.
As it can be gathered from the error on the determination of the central frequency ($\Delta\beta/\beta \sim 3 \times 10^{-8}$) a relative precision of $\sim 10^{-5}$ is at reach but it deteriorates down to a $\sim 10^{-4}$ level when extrapolated to higher energies.

The dependence on $\gamma^2$ in Eq.7 suggests the possibility of accelerating protons or heavy Ions to the final energies (6) to improve the accuracy, but the technical problems involved are quite considerable.

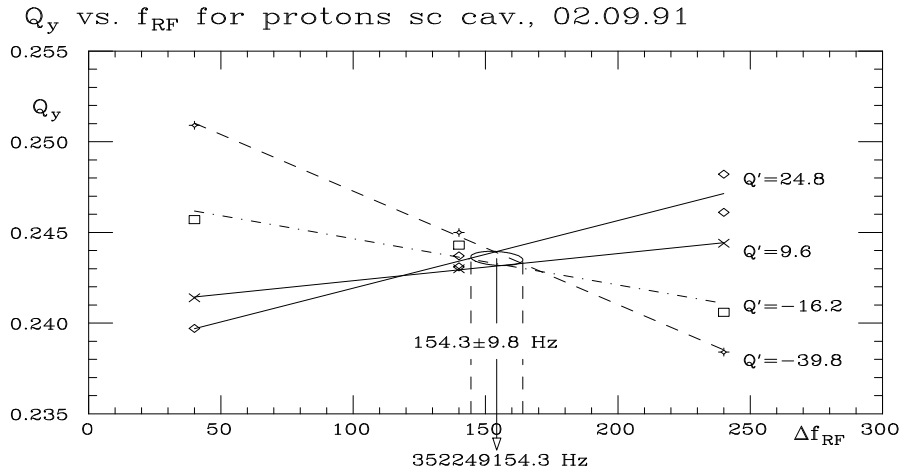


**Figure. 2**. *Proton* chromaticity measurements to determine the velocity and the *momentum* on the central orbit, ref.(5).

## SYNCHROTRON RADIATION IN THE VISIBLE RANGE

This method, based on the angular and energy dependence of synchrotron radiation distribution in storage rings (7), makes use of a special collimator housing two variable–amplitude slits to intercept portions of the distribution at two different positions in the vertical plane. The central beam energy is defined by the condition of transmitting the same photon flux in the two slits to be constructed and controlled to better than 0.1 $\mu$m.

The method, mainly applicable to beam transfer lines where special magnets can be inserted, also requires the knowledge of the dipolar field at the point of emission to a $\sim 5 \times 10^{-6}$ level. Even adopting the proposal of detecting the visible part of the emitted radiation to make use of optics to separate the narrow emission angles and avoid the limitations inherent to the use of X–rays techniques this method, quite elegant on paper, is of difficult realization.

## ELECTRON SCATTERING

Scattering of the bound electrons of hydrogen atoms in a gas target from *electrons* (Møller $e^-e^-$ scattering (8)) or *positrons* (Bhabha $e^+e^-$ scattering) offer another possibility of measuring the beam energy in a Storage Ring.

### Basic Møller Method

From the two body kinematic relation for elastic scattering on a target electron at rest the electron beam energy in units of the electron mass $m_e$

$$\frac{E_{\rm beam}}{m_e} = \left( \frac{8}{\theta^2(1-\kappa^2)} - 1 \right) \approx \left( \frac{8}{\theta^2(1-\kappa^2)} \right) \tag{8}$$

is determined from the momentum balance $\kappa = \cos\theta^*$ between the energies $E_{1,2}$ of the scattered electrons and the opening angle

$$\theta = \tan\theta_1 + \tan\theta_2 \tag{9}$$

The scattered electrons are detected in a near-symmetric configuration ($E_{1,2} \simeq E_{\rm beam}/2,\ \theta_1 \simeq \theta_2$) and the minimum opening angle ($\theta_1 = \theta_2,\ \kappa = 0$)

$$\theta_{\rm min} = \sqrt{\frac{8}{1 + E_{\rm beam}/m_e}} \approx \sqrt{\frac{8m_e}{E_{\rm beam}}} \tag{10}$$

typically ranges from 9.53 to 6.73 mrad for $E_{\rm beam} \in$ [45–90] GeV.
Calorimetric and/or geometric determinations of $E_{\rm beam}$ are possible depending on how the parameter $\kappa$ in Eq.8 is measured:

$$\kappa_A = \frac{E_{\rm beam} + m_e}{E_{\rm beam} - m_e} \frac{E_1 - E_2}{E_1 + E_2} \tag{11}$$

$$\kappa_B = \frac{\tan\theta_1 - \tan\theta_2}{\tan\theta_1 + \tan\theta_2} \tag{12}$$

A typical detector considered (9) for LEP2 would consist of:

- A hydrogen Gas Jet Target (GJT).
- A position-sensitive Silicon micro-strip detector.
- A high resolution Electro-Magnetic Calorimeter.
- A small silicon micro-strip detector in vacuum, close to the GJT, detecting recoil protons from elastic e-p scattering to monitor the spatial stability of the gas-$e^{\pm}$beam interaction area.

With a luminosity at the target electrons (8) of $4 \times 10^{31}$ cm$^{-2}$s$^{-1}$ the Møller rate is $\sim 2.2 \times 10^6$ events/hr and the statistical accuracy estimated for the LEP2 energies is of the order of 2 MeV in about 30 min.
The Bhabha scattering the cross section is about 1/4 of the Møller one and the associated statistical error two times larger for the same measuring time.

The scattering method provides on-line information on the beam energy **at the target location** [‡]. The extrapolation to the IP's requires careful monitoring of the horizontal orbit and the RF parameters.

## CALIBRATION BY RESONANT DEPOLARIZATION

### Transverse Polarization in $e^+e^-$ Storage Rings

Lepton beams circulating in Storage Rings become vertically polarized via the Sokolov-Ternov radiative polarization process (11): a small spin-flip probability associated to the quantum emission of synchrotron radiation has a large asymmetry in orienting the $e^+e^-$ magnetic moments along the guiding magnetic field in parallel/anti-parallel directions.

In an ideal accelerator the self-polarization mechanism builds up towards a theoretical asymptotic level $\hat{P} = 8/5\sqrt{3} = 92.4\%$ with a rise time

$$\tau_{ST} = c_{ST} \frac{\rho_{eff}^3}{\gamma^5} \quad , \quad c_{ST} = \frac{8}{5\sqrt{3}} \frac{m_e}{\hbar\, r_e} = 2.832 \times 10^{18} \text{ s m}^{-3} \tag{13}$$

where $r_e = e^2/m_e c^2$ is the electron classical radius and $\rho_{eff}$ is defined as(12)

$$(\rho_{eff}^3)^{-1} = \frac{1}{C} \oint \frac{ds}{\mid \rho(s) \mid^3} \tag{14}$$

Typical $\tau_{ST}$ values are:

$$\begin{aligned} \tau_{ST} &= 320 \text{ min /LEP1 at the } Z^0 \text{ energy} \\ &= 260\ (220) \text{ min /PEP II, LER (HER)} \end{aligned} \tag{15}$$

[‡] The beam energy varies along the beam path due to the localized compensation of synchrotron radiation losses in the RF stations (10) (energy sawtooth).

The dynamics of the spin vector $\vec{S}$ is determined by the particle magnetic history along the ring and described by the Thomas-BMT equation (13)(14):

$$\frac{d\vec{S}}{dt} = \vec{\Omega}_s \times \vec{S} \quad , \quad \vec{\Omega}_s = -\frac{e}{\gamma_e m_e}\left[(1+a_e\gamma_e)\vec{B}_\perp + (1+a_e)\vec{B}_{||}\right] \qquad (16)$$

where $a_e = (g-2)/2 = 1.159\,652\,188 \times 10^{-3}$ is the $e^+e^-$ gyro-magnetic anomaly and $\vec{B}_\perp, \vec{B}_{||}$ the field components transverse and parallel to the trajectory.

The effect of longitudinal fields on the spin precession frequency $\vec{\Omega}_s$ is $\gamma_e$ times weaker than that from transverse ones and in an ideal case where only vertical fields $\vec{B}_y$ are present the spin vector will precess around the stable solution $\vec{n}_0$ of Eq.16 parallel to $\vec{B}_y$ with a frequency $(a_e\gamma_e)$ times the cyclotron frequency $\Omega_c = -eB_y/m_e\gamma_e$.
The quantity $\nu = a_e\gamma_e$ measures the number of spin precessions in a machine revolution and in analogy with the terminology adopted for the betatron and synchrotron motion is called **spin tune**.
In a real machine *non vertical* magnetic fields on the particle trajectory originate from vertical misalignments in the quadrupoles and in the corrector dipoles used to compensate them, causing unwanted tilts to $\vec{n}_0$ and generating spurious vertical dispersion. As a consequence the orientation of the $\vec{n}_0$ vector becomes sensitive to energy fluctuations and dependent on the position of the particle along the ring due to quantum emission of radiation, reducing the degree of polarization (*spin-orbit coupling* (15)).

Refined orbit correction techniques known as *Harmonic Spin Matching* (*HSM*) have been conceived to compensate the tilt of the $\vec{n}_0$ vector by controlled spin rotations (16) generated by appropriate combinations of orbit bumps. The magnetic alignment of the machine elements and the quality of the orbit measurement are essential ingredients for a successful implementation of the *HSM* method. Beam-based techniques (17) to determine the relative offsets between quadrupoles and beam position monitors, associated with refined optical survey (18) and reliable beam orbit acquisition (19) proved to be extremely useful to implement the *HSM* method at LEP (20) and to improve the initial 10% polarization level (21) up to the 57% best result in 1993 (22).

## Polarimetry in Storage Rings

Laser polarimeters based on spin-dependent Compton scattering of circularly polarized photons on polarized electrons or positrons (23) have become a standard equipment in most $e^+e^-$ storage rings.
The differential Compton scattering cross section is (24)(25):

$$\frac{d\sigma}{d\Omega} = \frac{1}{2}\left(r_e\frac{k}{k_0}\right)^2\left[\Phi_0 + \Phi_1(\vec{\xi}) + \Phi_2(\vec{\xi},\vec{P})\right] \qquad (17)$$

where $k, k_0$ are the scattered and incident photon momenta in the $e^+e^-$ CM system, $\vec{P}$ the electron polarization vector and $\vec{\xi} \equiv (\xi_1, \xi_2, \xi_3)$ the photon polarization vector in terms of the normalized Stokes parameters ($\sum_{i=1}^{3} \xi_i = 1$).

When illuminating the beam with circularly polarized light [$\vec{\xi} \equiv (0, 0, \pm 1)$] the term $\Phi_1$ vanishes and Eq.17 shows an asymmetric behavior with respect to the helicity of the incoming photons via the term

$$\Phi_2(\vec{\xi}, \vec{P}) = -\xi_3 \left[ P_{||}\, F_1(k_0, k, \theta) + P_\perp\, F_2(k, \theta) \sin \phi \right] \tag{18}$$

where $\theta, \phi$ are the photon scattering angles.
Both recoil photons and/or leptons can be detected to measure the degree of polarization. When dealing with *longitudinally* polarized $e^+e^-$ beams the measured effect from a light helicity flipping $\xi_3 = \pm 1$ consists in a *backscattered rate* dependence. With *transverse* beam polarization the azimuthal asymmetry

$$A(\vec{P}, \vec{\xi}) = \frac{\Phi_2}{\Phi_0} = P_\perp\, \xi_3\, F(k_0, k, \theta) \sin \phi \tag{19}$$

produces an *up-down shift* in the mean $\tilde{y}$ of the vertical distribution of the high energy back-scattered photons, directly proportional to the degree of the polarization of both the photon and the $e^+e^-$ beams:

$$\Delta\tilde{y}(P_\perp, \xi_3, t) = \underbrace{\left( \kappa_{\rm pol}\, \xi_3\, \hat{P}\, \frac{\tau_{\rm eff}}{\tau_{\rm ST}} \right)}_{(\Delta\tilde{y})_\infty} [1 - \exp(-t/\tau_{\rm eff})] \tag{20}$$

The analyzing power $\kappa_{\rm pol}$ is calibrated by accurate determination of the effective rise time $\tau_{\rm eff}$ and the asymptotic mean-shift $(\Delta\tilde{y})_\infty$ from a fit to the time evolution (Eq.(20)) normalized to the actual light polarization state $\xi_3$.
The analyzing power of the LEP polarimeter (26)(27) is

$$\kappa_{\rm pol}^{\rm LEP} = (4.4 \pm 0.3)\ \mu{\rm m}/\%$$

and its global accuracy is $\sim 1\%$ in 1 minute data taking with 100% circularly polarized light.
Extreme care in producing and controlling the appropriate light polarization states is required to monitor very low $e^+e^-$ polarization levels.

## Resonant Depolarization (*RD*)

The **mean beam energy** of a storage ring can be determined to great accuracy by measuring the spin tune $\nu = a_{\rm e}\gamma_{\rm e}$ of a polarized $e^+e^-$ beam

$$\nu = N + \delta\nu = \left( \frac{a_{\rm e}}{m_{\rm e}c^2} \right) E_{\rm beam} = \frac{E_{\rm beam}}{0.4406486(1)} \tag{21}$$

where $m_e c^2/a_e = 440.6$ MeV is the energy change for a unitary spin tune change and the integer $N$ is known from magnetic measurements.
Typical spin tune values are:

$$\begin{aligned} \nu &= 103.469 \text{ at the } Z^0 \text{ energy} \\ &= 20.455 \text{ at PEP II / HER } (E_{beam} = 9.014 \text{ GeV}) \\ &= 7.046 \text{ at PEP II / LER } (E_{beam} = 3.105 \text{ GeV}) \end{aligned} \tag{22}$$

A frequency-controlled radial RF magnetic field makes the particle spin to precess away from the vertical axis and a depolarizing resonance occurs when the perturbing field oscillates at the spin precession frequency:

$$\omega_{dep}^{res} \equiv \Omega_s = 2\pi\, \delta\nu\, f_{rev} = 2\pi(1-\delta\nu)\, f_{rev} \tag{23}$$

The depolarizer frequency $f_{dep}^{res}$ at the resonance gives the fractional spin tune and the beam energy at the revolution frequency $f_{rev}$ (**actual** orbit):

$$E_{beam} = \nu \left(\frac{m_e c^2}{a_e}\right) = \left(N + \frac{f_{dep}^{res}}{f_{rev}}\right) \times 0.4406486 \text{ GeV} \tag{24}$$

The mirror ambiguity (*aliasing*) $f_{dep}^{res} = \delta\nu\, f_{rev} = (1-\delta\nu)\, f_{rev}$, typical of sampling data at equally spaced intervals (fig.3) is solved by determining the change in $f_{dep}^{res}$ when varying the beam energy through a known change in the RF frequency i.e. *without modifying the magnetic setup of the machine.*

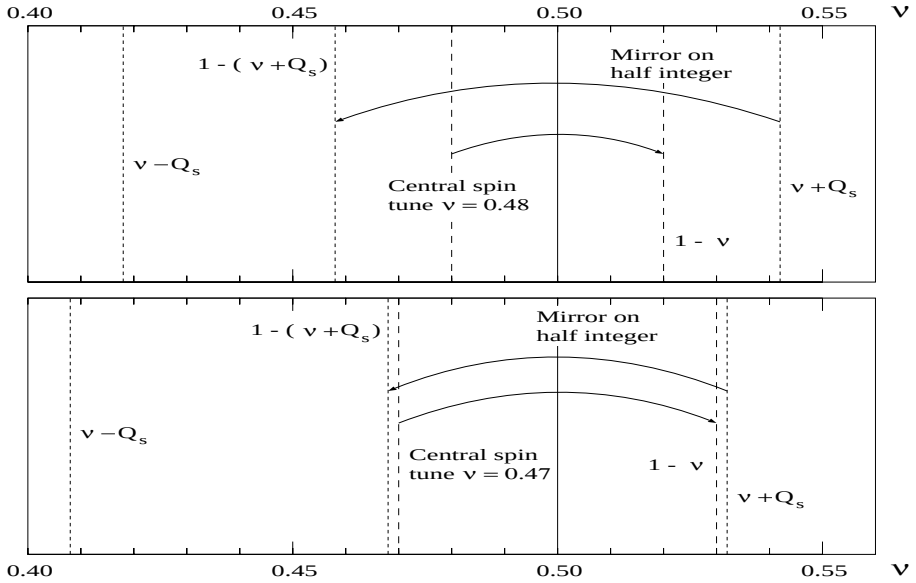


**Figure. 3**. Synchrotron satellites and mirror ambiguity (aliasing), ref.(20).

Resonant depolarization also occurs on synchrotron satellites $\delta\nu \pm Q_s$ of the main resonance. They can be separated from the latter as this is not shifted by a change in the synchrotron tune $Q_s$.

In practice the frequency of the depolarizer is slowly varied with time in steps over a given range until the polarization level drops to zero. The frequency step for which depolarization occurs defines the value of the spin tune interval and the step amplitude $\delta f_{\rm dep}$ gives the resolution of the spin tune and beam energy measurement. By properly gating the excitation of the perturbing field individual bunches can be selectively depolarized and the strategies meant to identify the true resonance can be applied while the re-polarization process of the previously depolarized bunches takes place.
An example of resonant depolarization is shown in fig.4.

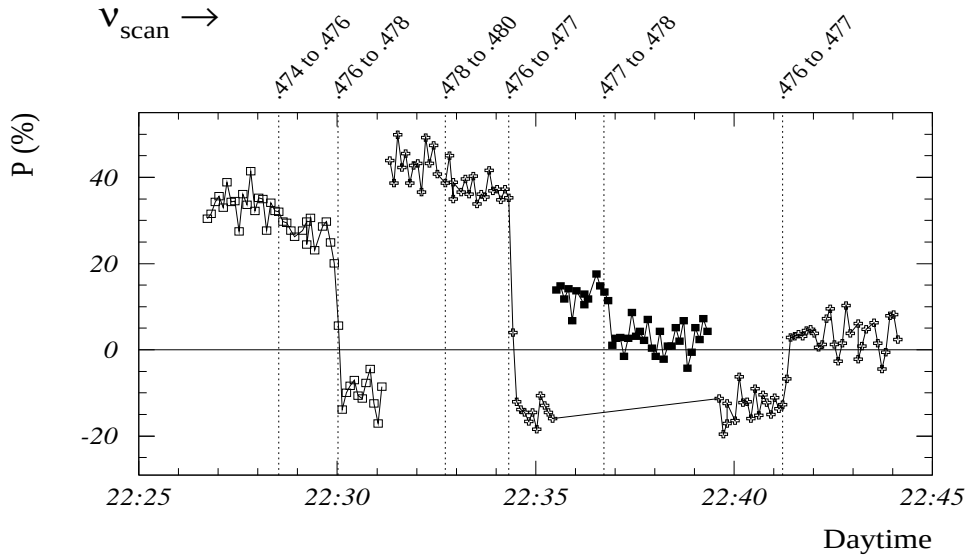


**Figure. 4**. Example of Energy Calibration with Resonant Depolarization. The upper scale shows the non–integer part of the spin tune corresponding to the sharp drop in the polarization level at the depolarizing resonance. Selective bunch depolarization is indicated by the different symbols. A partial spin–flip was checked to be real by flipping it back at the same spin tune (0.476–0.477), ref.(34).

Beam energy calibration by resonant depolarization was successfully implemented in LEP (28) and first applied in 1992 to reduce the systematic error on the mass of the $Z^0$ boson (29) [§].
In order to implement the *RD* method as close as possible to the accelerator operation conditions used for data taking the spin rotation induced by the experimental solenoids has to be compensated. The adopted scheme (30), first suggested in(31) (32), was experimentally verified (33) in 1992.

Following these results the *RD* method became the LEP standard energy calibration procedure (34) and routinely adopted at the end of physics fills during the three-point energy scan campaigns in 1993 (35) and 1995.

[§] From (29): $M_Z = (91.187 \pm 0.007)$ GeV.

The 1995 Calibration results (36) collected in fig.5 show the attained accuracies in the measurements of the beam energy and residual effects on the time evolution of the beam energy once the known perturbing mechanisms (see next section) are taken into account.

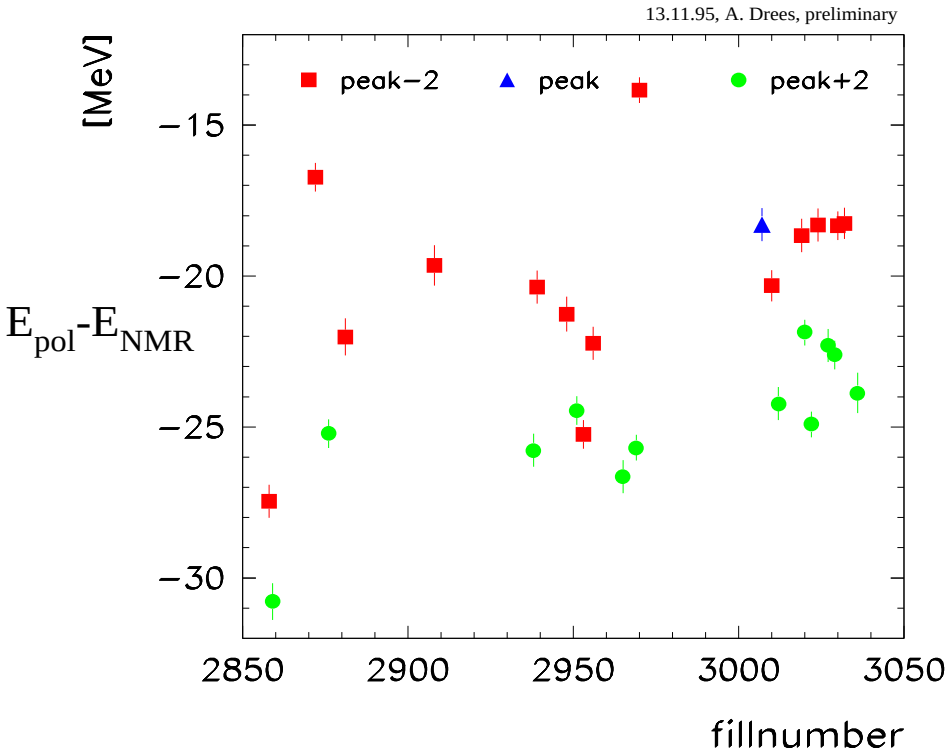


**Figure. 5**. Resonant Depolarization results from the 1995 LEP Run. The systematic shift $E_{\rm Pol} - E_{\rm NMR}$ between the beam energy from Resonant Depolarization and that estimated from NMR information shows a $\sim$ 9 GeV drift for both $E_{\rm e^{\pm}}^{\rm peak} \pm 2$ GeV beam energies over the 26 calibrated fills in the two month scan campaign, ref.(36).

## MECHANISMS CAUSING ENERGY CHANGES

Alignment tolerances in modern and future accelerators have become more and more critical with the introduction of strong focusing magnetic elements to contain beam phase space and with increasing beam currents implying precise positional requirements to reduce interactions of wake fields with the beam environment (37)(38). Besides occasional motion from seasonal variations of water content in the soil (39), natural micro-seismic disturbances and other effects, Earth tides are the major example of **periodic ground motion**.

## Terrestrial Tides

The equilibrium between the gravitational attraction of Moon and Sun on Earth and the centrifugal force between them all distorts the "spheroidal" surfaces of constant gravity solutions to Poisson's equation at the Earth surface. The result is a quadrupolar deformation of Earth crust producing two daily bulges with asymmetric amplitudes for any observer far from the Equator due to the inclination of the Earth rotational axis ($\epsilon_E = 23°26'$) and of the lunar orbital plane ($\epsilon_M = 5°08'$)to the ecliptic. As the Moon Transit time is longer than Earth day Lunar and Sun tides periods differ by 48 min 38 s, the global effect being additive in full/new moon configuration, subtractive in quadrature. The resulting Earth tides appear as a surface deformation with a period of 12 h 22 min, the amplitude of which depends on the observer latitude and on the Earth-Moon relative position. Maximum tides occur twice a month corresponding to *full* or *new moon* phases.

A wide spectrum of periodicities including ellipticity and oscillations of Earth and Moon orbits, equinox precession from Earth oblateness and other components makes the real picture much more complex (40)(41).
Two important observables are associated to the above phenomena, i.e. the *strain* and the *local gravity variations*.

The strain is a six-component second order tensor describing the **lateral motion** on Earth crust according to the local geological structure.

Gravity variations can be measured and predicted. Models using a Cartwright-Tayler-Edden (CTE) potential including up to 505 harmonic components are used in Geophysics and available in Centers for Earth Tides (42).

## Effects on Accelerators

Due to the crust strain the horizontal position of the magnetic elements in an accelerator changes periodically with time proportionally to the amplitude of the crust motion in the vertical direction (43). As a consequence the energy of particles circulating on the orbit defined by the *operational* RF frequency becomes *time-dependent* due to a additional bending strength from periodical off-axis passage in the quadrupoles.
Relative beam energy changes are related to strain-driven differences $\Delta C(t)$ between the lengths of the two orbits by the momentum compaction $\alpha_c$ :

$$\frac{\Delta E(t)}{E_0} = -\frac{1}{\alpha_c}\frac{\Delta C(t)}{C_0} = \kappa_{\rm tide}\ \Delta g(t) \tag{25}$$

where $\Delta g(t)$ is the time-dependent local gravity excursion and the tide coefficient $\kappa_{\rm tide}$ accounts for the coupling between strain and gravity changes. The sign convention in Eq.25 indicates that a positive strain (*expanding ring*) induces a *reduction* of the beam energy on the operational orbit with the usual notations above transition.

## The LEP TidExperiment

In a dedicated experiment (44) the evolution of the relative beam energy variation due to terrestrial tides has been measured at the LEP accelerator. A gravity excursion $\Delta g$ exceeding 140 $\mu$Gal [¶] occurs in the Geneva area during high tides and about 15% couples into transverse crust motion causing a variation of $\pm 0.5$ mm in the LEP circumference.

As shown in fig.6 a $\pm 100$ ppm relative energy excursion was measured in agreement with the behavior predicted from Eq.25 for the momentum compaction factor associated to the actual beam optics and also measured with the *RD* technique. A tide coefficient

$$\kappa_{\text{tide}} = (-0.86 \pm 0.08)\ \text{ppm}/\mu\text{Gal} \tag{26}$$

was determined from Eq.25 in good agreement with predictions (42).

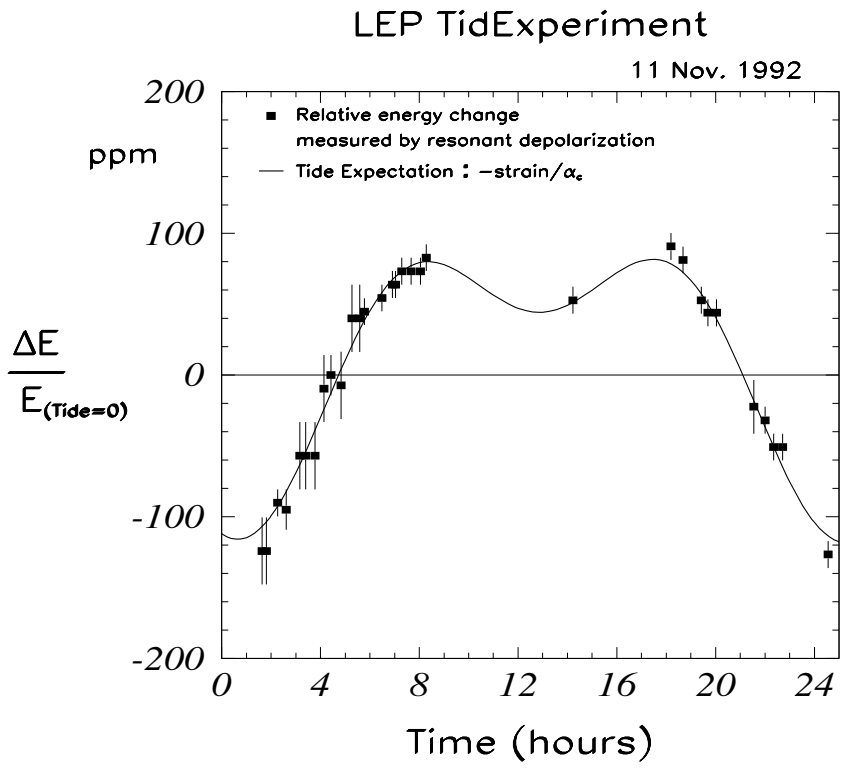


**Figure. 6**. Time evolution of the relative LEP beam energy variations driven by terrestrial tides measured over 24 hours. The solid line is calculated using the CTE tide model (41) with the tide coefficient from Eq.26, ref.(44).

[¶] 1 Gal = 1 cm $s^{-2}$ is the gravity acceleration unit adopted in geophysics (after G. Galilei).

### Environmental Perturbations (earth currents)

Variations of the LEP beam energy during a physics fill have been observed and traced back to changes in the bending field experienced by the beams as monitored by the two NMR probes available in 1995 in the tunnel (45).

Both exhibit drifts, steps and saturation as shown in the complex time behavior of fig.7 where the ordinate axis represents the *equivalent* beam energy as deduced from the measured field.
Short term perturbations of the order of 15 MeV together with long term shifts up to 10 MeV are likely to be driven by earth currents circulating along the LEP beam pipe which appear to be strongly correlated with electric current leaking into earth from the nearby railway system.

A clear correlation is shown in fig.8 between the time behavior of the rail voltage and that on the vacuum pipe, and the NMR-measured main bending field on the pole tips. Short term effects should not be seen by the beam due to the screening effect from the aluminum vacuum chamber.

The present understanding of the effect claims for parasitic currents not being directly responsible for the field changes but rather modulating the field in the magnets through mini-hysteresis loops.

A $1.7 \times 10^{-4}$ modulation of the main bending field applied in a few steps at the beginning of the fills seems to reduce the overall drift to about 3 MeV. This *conditioning* procedure has been adopted during the 1995 physics run as a partial cure to the effect.

## SUMMARY

An overview has been presented of methods adopted or suggested to perform absolute beam energy measurements in storage rings. Various techniques have been illustrated trying, when possible, to give a picture as complete as possible of both the achievable performance and the technical difficulties associated to them. Experimental results obtained at the LEP Storage Ring on the determination of the momentum on the central orbit using protons, and on the time evolution of the beam absolute energy during the 1995 Scan Campaign have been presented together with some interesting effects which affect the CM energy at the IP's by amounts well above the accuracies attainable with the adopted calibration methods.

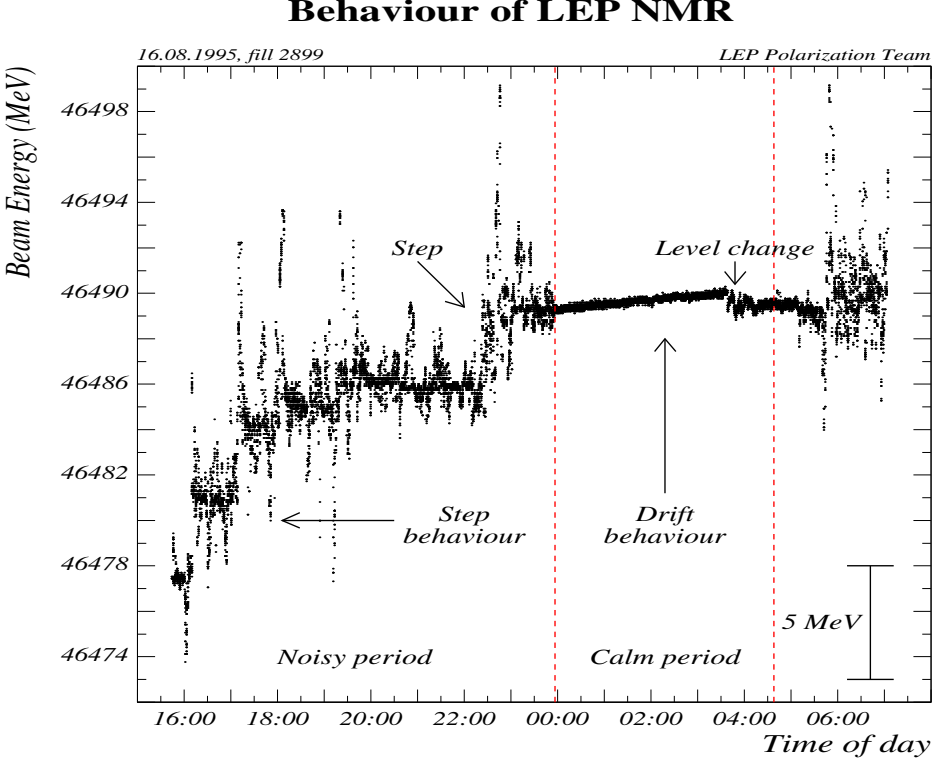


**Figure. 7**. Various changes in the LEP main bending field registered during a physics fill as detected by an NMR probe installed in one of the tunnel dipoles, ref.(45).

## ACKNOWLEDGMENTS

This review is the result of the collaboration with several working groups dealing with the problem of the beam energy monitoring and calibration.

The experimental results presented here are based on the work of many colleagues in the LEP Polarization Team, carried out over an extended period of time, during long MD shifts and endless nights in the control room.

It is a pleasure to give credit to the members of the Working Group on LEP Energy for the extensive work performed in the last years on the analysis of the large quantity of information collected in connection with the running of LEP for physics with the aim of understanding the several phenomena affecting the energy stability of the beams and produce a LEP Energy Model to be used to evaluate energy changes from logged variations in the main parameters of the accelerator.

Stimulating inputs from the Working Group on Energy Calibration as a subgroup of the 1995 Workshop on Physics at LEP2 are accounted for in the chapter on electron scattering.

Finally, the importance of the yearly Chamonix Workshop on LEP Performance as a forum for the continuous progress and evolution of the LEP Storage Ring is worth to be stressed and acknowledged.

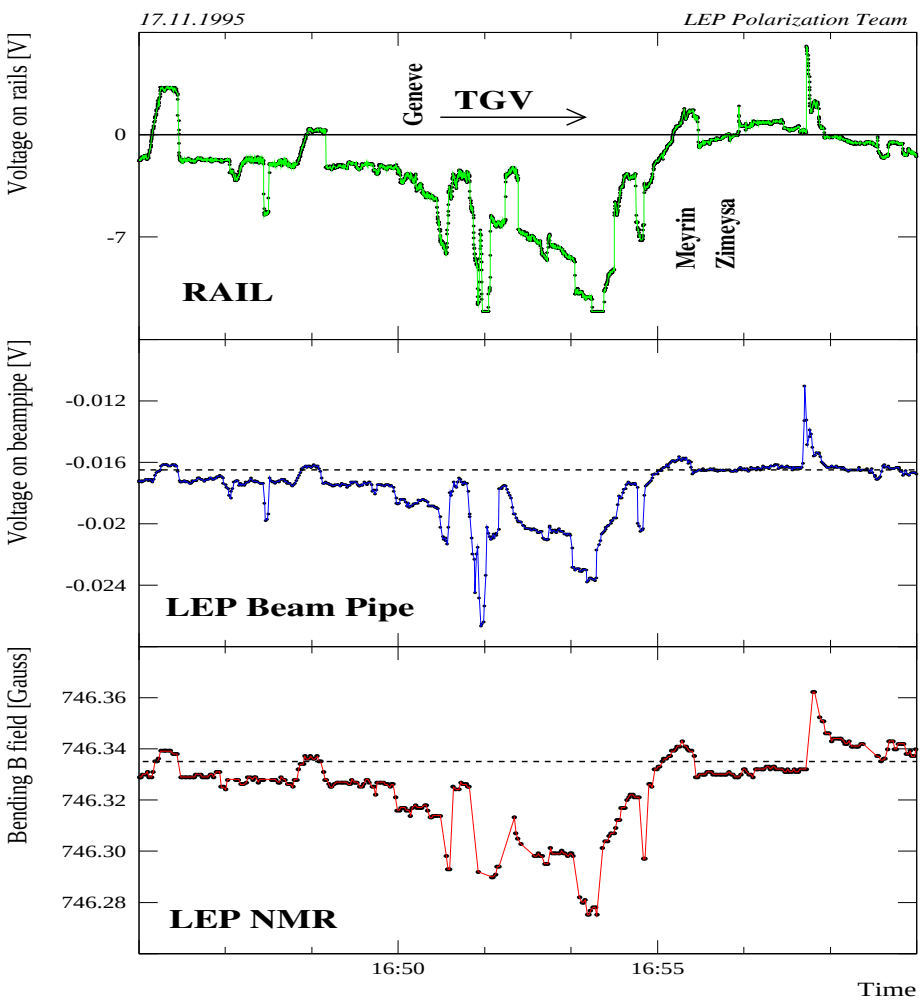


**Figure. 8**. Time correlation between voltage on rails, parasitic voltage on LEP vacuum chamber and the resulting main bending field variations, ref.(45).

## REFERENCES


1. J. Billan *et al.*, *Proc. XIV Int. Conf. on High Energy Accel., Tsukuba, Japan, August 1989*, and Particle Acc. 29 (1990) 215.
2. J. Billan *et al.*, *Proc. 1991 PAC, San Francisco, CA, May 1991.*
3. G.E. Fischer, CERN Accelerator School on Magnetic Measurements and Alignment, Montreux, Sept. 1992. CERN 92-05.
4. A. Hofmann and T. Risselada, CERN LEP Note 383, 1982.
5. R. Bailey *et al.*, "LEP Energy Calibration", *Proc. 2nd EPAC, Nice, France, June 12-16, 1990.*
6. D. Plane, Contribution to the WG4/Energy Calibration Subgroup, PHYSICS AT LEP2, CERN 96-01, vol 1, (Feb. 1996).
7. I.P. Karabekov, CEBAF PR-92-004 (March 1992) and CEBAF PR-93-009 (April 1993).
8. P. Galumian *et al.*, NIM **A 327** (1993) 269-276.
9. C. Cecchi, J.H. Field, T. Kawamoto and D. Schaile, Contribution to the WG4/Energy Calibration-Subgroup, PHYSICS AT LEP2, CERN 96-01, vol 1, (Feb. 1996).
10. M. Bassetti, *Proc. 11th Int. Conf. on High Energy Accelerators, Geneva, Switzerland, July 7-11, 1980.*
11. A.A. Sokolov and I.M. Ternov, Sov. Phys. Dokl. 8 (1964) 1203.
12. M. Böge, private communication.
13. L.H. Thomas, Philos. Mag. 3 (1927) 1.
14. V. Bargmann, L. Michel and V.L. Telegdi, Phys. Rev. Lett. 10 (1959) 435.
15. Ya.S. Derbenev and A.M. Kondratenko, Sov. Phys. JETP **37** (1973) 968.
16. R. Rossmanith and R. Schmidt, NIM **A 236** (1985) 231.
17. I. Barnett *et al.*, "Dynamic Beam Based Calibration of Orbit Monitors at LEP", *Proc. 4th Int. Workshop on Accelerator Alignment, Tsukuba, Japan, Dec. 1995*, KEK Proc. 95-12 and CERN-SL/95-97 (BI).
18. M. Mayoud and A. Verdier, "Survey and correction of LEP elements", *Proc. 3rd Workshop on LEP Performance*, J. Poole ed., CERN-SL/93-19-DI, (Feb. 1993).
19. J. Borer, "BOM system hardware status", *Proc. 3rd Workshop on LEP Performance*, J. Poole ed., CERN-SL/93-19-DI, (Feb. 1993).
20. R. Assmann, "Transversale Spin-Polarisation und ihre Anwendung für Präzisionmessungen bei LEP", PhD Thesis, 1994.
21. L. Knudsen *et al.*, "First Evidence of Transverse Polarization In LEP", *Proc. Symp. High Energy Spin Physics, Bonn, Germany, Sept. 1990.*
22. M. Placidi *et al.*, "Lepton Beam Polarization at LEP", *Proc. Int. Symposia on H. E. Spin Physics and Polarization Phenomena in Nuclear Physics, (SPIN '94), Bloomington, Indiana, U.S.A., Sept. 15-22, 1994.*
23. V.N. Baier and V.A. Khoze, Sov. J. Nucl. Phys. 9 (1969) 238.
24. U. Fano, J. Opt. Soc. Am 39 (1949) 859.
25. F.W. Lipps and H.A. Toelhoek, Physica, XX (1954) 85 and 395.
26. M. Placidi and R. Rossmanith, NIM **A 274** (1989) 79.

27. B. Dehning, "Elektronen- und Positronen-Polarisation im LEP-Speicher ring und Präzisionsbestimmung der Masse des Z-Teilchens", PhD Thesis, 1996.
28. L. Arnaudon *et al.*, Phys. Lett. **B 284** (1992) 431.
29. The Working Group on LEP Energy and the LEP Collaborations ALEPH, DELPHI, L3 and OPAL: Phys. Lett. **B 307** (1993) 187.
30. A. Blondel, LEP-Note 629 (1990).
31. K. Steffen, Int. Report DESY PET-82 (1982), unpublished.
32. R. Rossmanith, LEP-Note 525 (1985).
33. M. Placidi, "Polarization Results and Future Perspectives", *Proc. 3rd Workshop on LEP Performance*, J. Poole ed., CERN-SL/93-19-DI, (Feb. 1993).
34. L. Arnaudon *et al.*, "Accurate determination of the LEP beam energy by resonant depolarization", Z. Phys. **C 66**, 45-62 (1995).
35. They Working Group on LEP Energy, "The Energy Calibration of LEP in the 1993 scan", Z. Phys. **C 66**, 567-582 (1995).
36. A. Drees, "LEP Beam Energy Calibration in 1995", *Proc. XXXIst Rencontres de Moriond, "Electroweak Interactions and Unified Theories", Les Arcs, France, March 16-23, 1996.*
37. G.E. Fischer, SLAC-PUB-3392 Rev., July 1985.
38. G.E. Fischer, *Proc. First Int. Workshop on Accelerator Alignment, SLAC, July 1989* and SLAC-375.
39. J. Wenninger, "Study of the LEP Beam Energy with Beam Orbits and Tunes", CERN-SL/94-14 (BI), 1994.
40. K.E. Lang, Astrophysical Formulae, 2nd Edition, Springer Verlag.
41. P. Melchior, "The Tides of the Planet Earth", 2nd Edition, Pergamon Press, 1983.
42. Code provided by Prof. P. Melchior from International Center for Earth Tides, Bruxelles, Belgium.
43. G. Fischer and A. Hofmann, *Proc. 2nd Workshop on LEP Performance*, J. Poole ed., CERN-SL/92-29-DI, (Feb. 1992).
44. L. Arnaudon *et al.*, "Effects of terrestrial tides on the LEP beam energy", NIM **A 357** (1995) 249-252.
45. M. Geitz, "Investigations on environmental effects of the beam energy – magnetic field perturbations", Diploma Thesis, 1996.